Atmos. Chem. Phys., 13, 3695–3703, 2013
www.atmos-chem-phys.net/13/3695/2013/
doi:10.5194/acp-13-3695-2013

Atmospheric Chemistry and Physics Open Access

Exploring the atmospheric chemistry of $O_2SO_3^-$ and assessing the maximum turnover number of ion-catalysed H_2SO_4 formation

N. Bork[1,2], **T. Kurtén**[1,3], **and H. Vehkamäki**[1]

[1]Division of Atmospheric Sciences and Geophysics, Department of Physics, University of Helsinki, P.O. Box 64, 00014 University of Helsinki, Finland
[2]Department of Chemistry, H.C. Ørsted Institute, University of Copenhagen, 2100, Copenhagen Ø, Denmark
[3]Laboratory of Physical Chemistry, Department of Chemistry, P.O. Box 55, University of Helsinki, 00014 University of Helsinki, Finland

Correspondence to: N. Bork (nicolai.bork@helsinki.fi)

Received: 24 August 2012 – Published in Atmos. Chem. Phys. Discuss.: 22 November 2012
Revised: 4 March 2013 – Accepted: 14 March 2013 – Published: 4 April 2013

Abstract. It has recently been demonstrated that the $O_2SO_3^-$ ion forms in the atmosphere as a natural consequence of ionizing radiation. Here, we present a density functional theory-based study of the reactions of $O_2SO_3^-$ with O_3. The most important reactions are (a) oxidation to $O_3SO_3^-$ and (b) cluster decomposition into SO_3, O_2 and O_3^-. The former reaction is highly exothermic, and the nascent $O_3SO_3^-$ will rapidly decompose into SO_4^- and O_2. If the origin of $O_2SO_3^-$ is SO_2 oxidation by O_3^-, the latter reaction closes a catalytic cycle wherein SO_2 is oxidized to SO_3. The relative rate between the two major sinks for $O_2SO_3^-$ is assessed, thereby providing a measure of the maximum turnover number of ion-catalysed SO_2 oxidation, i.e. how many SO_2 can be oxidized per free electron. The rate ratio between reactions (a) and (b) is significantly altered by the presence or absence of a single water molecule, but reaction (b) is in general much more probable. Although we are unable to assess the overall importance of this cycle in the real atmosphere due to the unknown influence of CO_2 and NO_x, we roughly estimate that ion-induced catalysis may contribute with several percent of H_2SO_4 levels in typical CO_2-free and low NO_x reaction chambers, e.g. the CLOUD chamber at CERN.

1 Introduction

One of the most significant uncertainties in weather and climate forecasts is related to the processes leading to cloud formation (Simpson and Wiggert, 2009; Rosenfeld, 2006; Spracklen et al., 2008; Carslaw et al., 2002). It is well known that each cloud droplet forms around a cloud condensation nucleus (CCN). CCNs may well originate from a solid particle (e.g. soot, salt, or pollen), but recently it has become increasingly clear that a significant part originate from clustering of purely gaseous molecules (Kulmala et al., 2004; Wiedensohler et al., 2009; Yu and Luo, 2009; Kazil et al., 2010).

Although molecular clustering and aerosol particle formation has been intensively studied, fundamental uncertainties prevail. One of the most significant uncertainties concerns the chemical composition of the very smallest molecular clusters. Sulfuric acid has repeatedly been found in atmospheric clusters, and the concentration of sulfuric acid is known to correlate well with nanoparticle formation rates (Sipilä et al., 2010; Nieminen et al., 2009). Traditionally, binary nucleation of H_2SO_4 and H_2O has been the most studied mechanism, but during the last couple of decades it has become evident that a third species (e.g. ammonia or an amine) is needed as well (Kirkby et al., 2011; Ortega et al., 2012). However, the critical importance of sulfuric acid remains undisputed.

The main source of atmospheric sulfuric acid is UV-induced oxidation of SO_2, which is emitted from volcanoes and through fossil fuel combustion. The oxidation mechanism involves several elementary reactions, but is relatively well understood (Bondybey and Beyer, 2002). The rate limiting step is the initial S(IV) to S(V) oxidation (Li and McKee, 1997):

$$SO_2 + OH + M \rightarrow HSO_3 + M, \quad \text{(R1)}$$

where M is a stabilizing molecule. HSO_3 is then further oxidized to SO_3 by O_2 before hydration to H_2SO_4. The final hydration is known to be catalysed by one or more excess water molecules and is the main sink of atmospheric SO_3 (Morokuma and Muguruma, 1994). In addition to this, a mechanism where SO_2 is oxidized by Criegee biradicals has been proposed (Welz et al., 2012; Mauldin III et al., 2012).

During the last decades, the influence of ions in aerosol formation has been targeted by several chamber studies (Kirkby et al., 2011; Enghoff and Svensmark, 2008). Here, it has been firmly established that ions enhance formation of nanometer-sized aerosol particles in SO_2- and O_3-containing atmospheres under UV exposure. One possible explanation, based on classical nucleation theory, is that the energy barrier of nucleation is lowered by the charge hereby increasing the total nucleation rate (Tohmfor and Volmer, 1939; Lovejoy et al., 2004). The lower barrier might result from reduced evaporation rates from ionic clusters due to charge delocalization or from increased collision rates between ionic particles and dipolar molecules or between oppositely charged particles (Su and Bowers, 1973; Kupiainen et al., 2012).

A fundamentally different approach to explain ion-induced nucleation is through ion-induced chemistry altering the composition of the metastable gas phase. This idea is supported by several experimental studies where mainly collision-limited ionic gas-phase chemical reactions were found; see e.g. Fehsenfeld and Ferguson (1974) and references therein. Further, a successful chamber study led Svensmark et al. (2007) to suggest an ion-induced SO_2 oxidation mechanism. Despite of this, little research has been dedicated to enhanced nucleation from ion-induced chemistry; see however Sorokin and Arnold (2007, 2009) and Enghoff et al. (2012).

Atmospheric ions are mainly products of radioactivity and galactic cosmic rays. Although both cations and free electrons are produced, most attention has gathered around the influence of the electrons and subsequent anions (Nadykto et al., 2006; Kurtén et al., 2009). It is well known that some of the first stable products are $O_2^-(H_2O)_m$ and $O_3^-(H_2O)_n$ clusters (Luts and Parts, 2002). The first 5 water molecules are strongly bound to the ion, but several more may attach under cold and/or humid conditions (Bork et al., 2011b).

Further, it has been shown that $O_3^-(H_2O)_n$ may oxidize SO_2 to SO_3^- via the reaction

$$O_3^-(H_2O)_n + SO_2 \rightarrow SO_3^-(H_2O)_n + O_2. \quad \text{(R2)}$$

This reaction is probably the dominant sink of O_3^- in most reaction chambers since CO_2 most often is omitted. Initially, the product cluster might partially decompose due to the large release of internal energy in the oxidation. However, the high concentrations of both O_2 and H_2O ensure that the equilibrium quickly settles. Hereafter, the predominant products

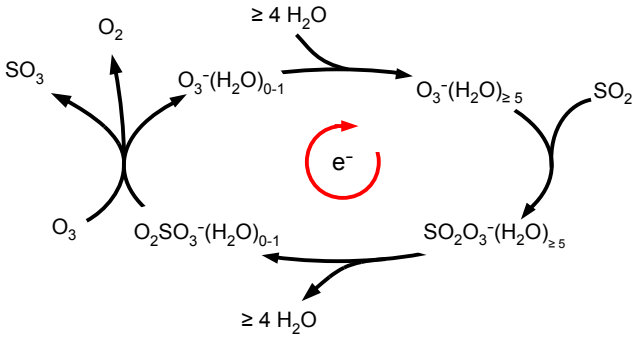

Fig. 1. Schematic of a simple catalytic SO_2 oxidation cycle. The net reaction is $O_3 + SO_2 \rightarrow O_2 + SO_3$, and the catalyst is the electron. All reaction rates are mainly collision-limited.

are $O_2SO_3^-$ and $O_2SO_3^-(H_2O)$ (Bork et al., 2011a; Möhler et al., 1992). This is supported by a recent field study by Ehn et al. (2010), finding that, after HSO_4^-, $O_2SO_3^-$ is the second most common sulfur-based anion in a boreal forest.

The further chemical fate of $O_2SO_3^-$ and the extra electron is largely unknown, but is potentially important. We have investigated the most probable reactions of de- and monohydrated $O_2SO_3^-$ under standard conditions focusing mainly on the reaction with O_3. The two main reactions are

$$O_2SO_3{}^-W_{0-1} + O_3 \rightarrow \begin{cases} O_3SO_3{}^-W_{0-1} + O_2 & \text{(a)} \\ O_3{}^-W_{0-1} + O_2 + SO_3 & \text{(b)} \end{cases} \quad \text{(R3)}$$

where W is shorthand for water. The latter reaction is of particular interest since a catalytic cycle of SO_2 oxidation thereby is closed (see Fig. 1).

Using ab initio calculations we have determined the structures, energies and thermodynamics of reactants, transition states and products. We proceed to evaluate the rates of the relevant reactions and hereby evaluate the total turnover number, i.e. how many SO_2 oxidations a single electron on average will induce. Finally, we estimate the maximum fraction of H_2SO_4 originating from ionic catalysis under typical conditions in CO_2-free reaction chambers.

2 Computational details

As always when treating weakly bound systems, anionic systems and radical reactions, special care must be taken to ensure reliable results. Of special interest of this study is the relative adiabatic electron affinity of SO_3 and O_3 since this energy difference will be the thermodynamic driving force behind Reaction (R3b). The experimental electron affinity of O_3 has been determined to 202.9 kJ mol^{-1} with high certainty (Novick et al., 1979; Arnold et al., 1994). On the contrary, despite several studies, the electron affinity of SO_3 remains highly uncertain. The most recent studies find values of 183 ± 10 kJ mol^{-1} (Gleason, 1987) and 190 ± 10 kJ mol^{-1} (Dobrin et al., 2000) suggesting that, most likely, the electron affinity of O_3 exceeds that of SO_3 by ca. 15 kJ mol^{-1}.

While scanning a variety of methods, we found that most ab initio methods actually predict a larger electron affinity of SO_3 than of O_3, despite large basis sets. However, the CAM-B3LYP functional is an exception to this (Yanai et al., 2004). At basis sets of at least triple zeta quality, both the order and magnitude of the electron affinity difference are in accordance with the experimental value. Therefore, we have used the CAM-B3LYP functional with aug-cc-pVTZ basis set throughout (Dunning, 1989), predicting an electron affinity difference between O_3 and SO_3 to be $18\,\mathrm{kJ\,mol^{-1}}$. We note that adding further *d* functions, as normally preferable for third period elements, is not desirable since we found that the otherwise accurate aug-cc-pV(T+d)Z basis set predicted the electron affinity difference to $-35\,\mathrm{kJ\,mol^{-1}}$. Further, it has been shown that CAM-B3LYP is superior to B3LYP with respect to determining activation energies for a range of typical chemical reactions (Peach et al., 2006; Yanai et al., 2004; Elm et al., 2012). All density function theory (DFT) calculations were performed using the Gaussian09 package (http://gaussian.com/), and all clusters were corrected for basis set superposition error using the counterpoise method (Boys and Bernardi, 1970).

The present reactions involve both neutral and charged ozone as well as highly oxidized sulfur species with unknown electronic properties. Therefore, we have performed CCSD(T)-F12 calculations with the VDZ-F12 basis set to test the DFT results (Adler et al., 2007; Peterson et al., 2008). These calculations have been performed using the MOLPRO package (http://molpro.net/) and are described in detail elsewhere (Bork et al., 2011b).

Energy barriers were determined by scans of the potential energy surface and confirmed by frequency analyses showing exactly one imaginary frequency. Further, by following the reaction coordinate in both directions, it was ensured that transition states indeed connected the desired reactants and products.

The temperature-dependent reaction rate constants, $k(T)$, were determined using harmonic transition state theory (Hänggi et al., 1990; Billing and Mikkelsen, 1996):

$$k(T) = A \times \exp\left(\frac{-E_\mathrm{A}}{RT}\right), \text{ where} \quad (1)$$

$$A = \frac{\prod \nu_\mathrm{reac}}{\prod \nu_\mathrm{TS}^\dagger}. \quad (2)$$

E_A is energy barrier separating reactants and products, R the molar gas constant and ν the harmonic frequencies for the reactant and transition state. The † indicates that the imaginary frequency should be omitted.

We finally stress that all reactants and products are radicals and hence electronic doublets. In all cases, molecular oxygen is treated as an electronic triplet but, due to the pairing with the doublet state of the ionic radical, all reactions are spin-allowed. Further, none of the considered pre-reactive complexes contains any symmetry.

3 Results and discussion

3.1 Self dissociation

The simplest reaction of $O_2SO_3^-$ based clusters is spontaneous dissociation into O_2 and SO_3^-:

$$O_2SO_3^-W_{0-1} \rightleftharpoons SO_3^-W_{0-1} + O_2. \quad (R4)$$

This reaction is potentially important since the reaction

$$SO_3^-W_{0-1} + O_3 \rightarrow SO_3 + O_3^-W_{0-1} \quad (R5)$$

is distinctly exothermic, thus providing a direct path to complete the catalytic cycle in Fig. 1. Further, both SO_3^- and $O_2SO_3^-$ have recently been measured by Ehn et al. (2010) in a Finnish boreal forest, where typical ratios of 1 : 10 were found, suggesting that this reaction may be significant.

After optimizing all species we found free O_2 binding energies of 48.9 and $39.8\,\mathrm{kJ\,mol^{-1}}$ for the de- and monohydrated clusters at standard conditions, respectively. Little experimental data is available, but Möhler et al. (1992), based on mass spectrometrical data, concluded that O_2 is bound stronger to SO_3^- than H_2O is to CO_3^-, HCO_3^-, and NO_3^-. This implies that $\Delta G^\circ_{(R4)} \leq -25\,\mathrm{kJ\,mol^{-1}}$ at room temperature (Keesee et al., 1979; Payzant et al., 1971).

These binding energies suggest much lower $[SO_3^-]:[O_2SO_3^-]$ ratios than the observed ratio of 1 : 10. Although several factors may contribute to this discrepancy, it appears most likely that SO_3^- may be stabilized in configurations not considered here, preventing $O_2SO_3^-$ formation. Some of the most obvious candidates include OH, HO_2, other radicals, and/or clusters containing more than one water. It is well known that weakly bound clusters may evaporate inside spectrometers. In accordance with this, it seems that the reported field-based concentrations of unclustered SO_3^- are overestimated.

We conclude that, although some SO_3^- exists, the population of $O_2SO_3^-$ is significantly higher and we will thus focus on this species in the remainder of this article. Finally, we note that, contrary to previous studies, we generally avoid referring to $O_2SO_3^-$ as SO_5^- since the $O_2-SO_3^-$ bond resembles that of a molecular cluster more than a molecular covalent bond, concerning both distance and strength.

3.2 O_3 collision and formation of $O_2SO_3^-W_{0-1}\cdot O_3$

First, the $O_2SO_3^-\cdot O_3$ and $O_2SO_3^-\cdot W\cdot O_3$ molecular complexes were optimized (see Fig. 2). In the dehydrated system, only a few different stable configurations were found, while at least 10 stable configurations were found in the monohydrated cluster. Most configurations were within $10\,\mathrm{kJ\,mol^{-1}}$ and are thus predicted to co-exist at typical atmospheric temperatures. However, for the remainder of this article, mainly the single most stable configurations with respect to ΔG° will be considered.

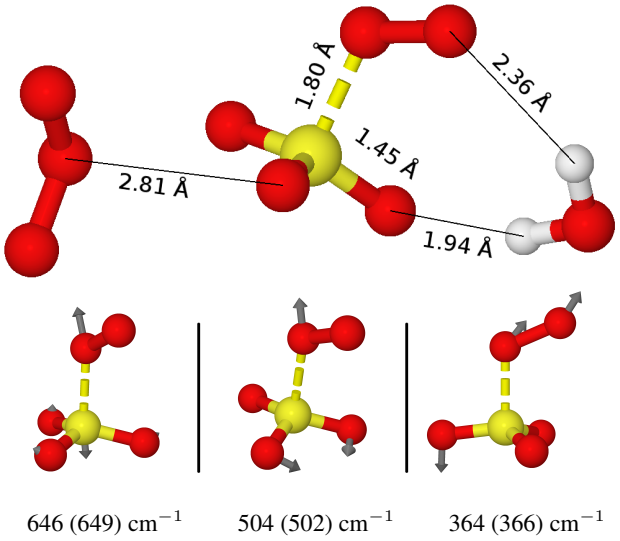

Fig. 2. Top: the molecular complex between $O_2SO_3^-$, H_2O and O_3 including some descriptive bond lengths. Removing either the H_2O or O_3 causes little structural rearrangement. Bottom: directions and frequencies of the three normal vibrational modes along the $SO_3^- - O_2$ bond in the dehydrated (monohydrated) cluster. Sulfur is yellow, oxygen red, and hydrogen white.

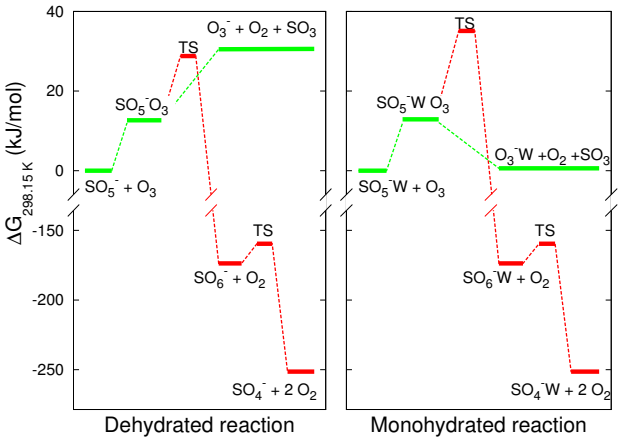

Fig. 3. Schematic overview of the Gibbs free energy of the relevant species at standard conditions. The barrier height for $O_2SO_3^-$ oxidation is increased by ca. 6 kJ mol^{-1} by the presence of a water molecule while the thermodynamics of charge transfer and cluster decomposition is changed from distinctly endothermic to almost thermoneutral. At standard conditions and 50 % relative humidity, ca. 90 % of $O_2SO_3^-$ is monohydrated.

Structurally, only small changes were apparent upon ozonation since the binding preferences of the O_3 and H_2O are very different. In accordance with this, the binding energy of O_3 to $O_2SO_3^-$ is only minutely affected by hydration. Considering the equilibrium,

$$O_2SO_3^-\,W_{0-1} + O_3 \leftrightharpoons O_2SO_3^-\,W_{0-1}O_3. \qquad \text{(R6)}$$

Regardless of the presence or absence of water, we found $\Delta H_{(R6)}$ values of ca. -12 kJ mol^{-1} and $\Delta G^\circ_{(R6)}$ values of ca. $+12$ kJ mol^{-1} implying a short lifetime towards de-ozonation since no energy barrier is present. See Ortega et al. (2012) for a description of the link between binding energies and lifetime.

Neither does the water molecule change the thermodynamics of ozonation, nor does the ozone change the thermodynamics of hydration. Considering the condensation–evaporation equilibrium, i.e.

$$O_2SO_3^-\,(O_3)_{0-1} + W \leftrightharpoons O_2SO_3^-\,(O_3)_{0-1}W, \qquad \text{(R7)}$$

we find $\Delta H_{(R7)}$ and $\Delta G^\circ_{(R7)}$ of -42 and -7 kJ mol^{-1}, respectively. Also this reaction was investigated by Möhler et al. (1992), who determined $\Delta G^\circ_{(R7)}$ to -17.2 kJ mol^{-1}. To clarify this discrepancy, we optimized all relevant species with CCSD(T)-F12 and found an electronic binding energy of 51.3 kJ mol^{-1}. Assuming $\Delta S_{(R7)} = -120$ J mol^{-1} K^{-1}, which is typical of water condensation reactions, we find $\Delta G^\circ_{(R7)} = -15$ kJ mol^{-1}, in good accordance with Möhler et al. (1992).

Using the law of mass action,

$$\frac{[O_2SO_3^-\,W]}{[O_2SO_3^-]} = [W] \times \exp\left(\frac{-\Delta G}{RT}\right), \qquad (3)$$

we find that roughly 90 % of $O_2SO_3^-$ are hydrated at $T = 298$ K and 50 % relative humidity, and the fate of the hydrated cluster is thus of primary importance. However, in all but extremely dry conditions both hydrated and dehydrated clusters co-exist and should both be considered when evaluating Reactions (R3a) and (R3b).

Having established the structures and relative populations of the relevant clusters, we proceed to evaluate the possible chemical reactions.

3.3 Cluster decomposition

The most important reaction considered here is decomposition of the reactant cluster as

$$O_3{\cdot}O_2SO_3^-\,W_{0-1} \rightarrow O_3^-\,W_{0-1} + O_2 + SO_3. \qquad \text{(R8)}$$

As mentioned, the Gibbs free binding energy of the $O_2SO_3^-$ cluster is at least 25 kJ mol^{-1}, which is only partially compensated by the transferring of the electron, and the dehydrated Reaction (R5) is ca. 15 kJ mol^{-1} exothermic.

However, the water molecule is bound significantly stronger to the O_3^- ion than to the SO_3^- ion. Considering also this effect we find that the monohydrated cluster decomposition reaction is ca. 10 kJ mol^{-1} exothermic at $T = 298$ K. The Gibbs free potential energy surface is shown in Fig. 3 for $T = 298$ K and tabulated in the Supplement.

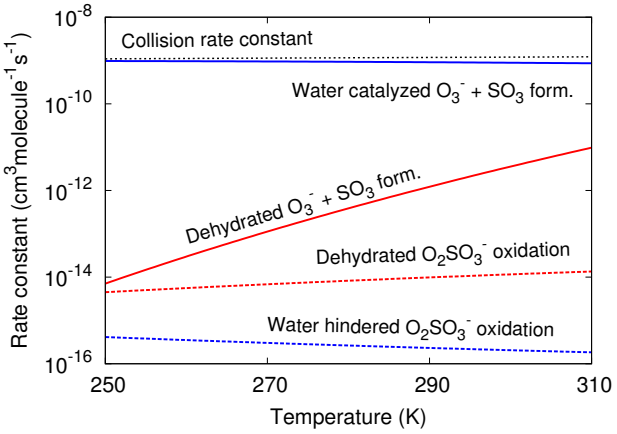

Fig. 4. Bimolecular rate constants of cluster decomposition mechanism and $O_2SO_3^-$ oxidation in $cm^3\,molecule^{-1}\,s^{-1}$ as function of temperature. For both the dehydrated and the monohydrated systems, cluster breakup is favoured although much more so in the hydrated systems. At standard conditions and 50 % relative humidity, ca. 90 % of $O_2SO_3^-$ is monohydrated. The collision rate constant with O_3 is indicated (50 % relative humidity).

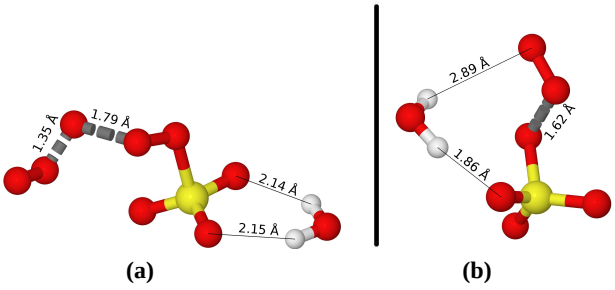

Fig. 5. Transition states for **(a)** the oxidation of $O_2SO_3^-W$ to $O_3SO_3^-W$ and **(b)** the following dissociation to SO_4^-W. The active bonds are shown as broken grey, and some descriptive bond lengths are indicated. Sulfur is yellow, oxygen red and hydrogen white.

Considering first the dehydrated reaction, we identified three vibrational modes of the $O_2SO_3^-O_3$ clusters clearly leading towards dissociation via

$$O_2SO_3^- \rightarrow O_2 + SO_3^-. \qquad \text{(R9)}$$

These modes are shown in Fig. 2. All modes will be active at all times, and their combined magnitude at time, t, is given by $f(t) = \sum_{\nu=(646\,cm^{-1},504\,cm^{-1},364\,cm^{-1})} d_\nu \cos(\nu t)$, where d_ν is the displacement vector of vibration ν. Assuming that all modes are all in their ground states and that their displacement vectors are of similar magnitudes, we find an effective frequency of 540 cm^{-1} by functional analysis of $f(t)$.

By analysing the Mulliken charges (Mulliken, 1955) during these vibrations, it was confirmed that electronic density was smoothly being transferred to O_3 from SO_3^- during a vibration and that no electronic barrier separated the charge transfer Reaction (R5). Hence, the minimum energy required to dissociate the dehydrated cluster is exactly the energy of the net reaction, here 30.5 $kJ\,mol^{-1}$ above the reactants. This implies an overall rate constant of 2.9×10^{-12} $cm^3 molecule^{-1} s^{-1}$ at $T = 298$ K (see also Fig. 4).

Contrary to the dehydrated cluster, in the monohydrated cluster the dissociation into SO_3, O_2, and O_3^-W is almost thermoneutral. In this case the rate limiting step is formation of the O_3 $O_2SO_3^-W$ cluster itself and the effective barrier is hence just 12.9 $kJ\,mol^{-1}$ at 298 K. The mechanism leading to cluster decomposition is however identical to the dehydrated cluster, and the modes leading to dissociation are almost identical. These are given in parentheses in Fig. 2. Due to the small energy barrier, we find that this reaction essentially is collision-limited (see also Fig. 4).

Comparing the decomposition rates of the dehydrated and monohydrated systems, we see that the water molecule is significantly facilitating cluster decomposition. The main reason is the more favourable thermodynamics since H_2O is bound significantly stronger to O_3^- than to $O_2SO_3^-$.

3.3.1 Formation of $O_3SO_3^-$

The other major reaction sink of $O_2SO_3^-$ considered here is oxidation by O_3. The sulfur is already tetrahedrally coordinated by oxygen, so the only possible oxidation is from further O–O binding. Most likely is the formation of $O_3SO_3^-$ since the reaction

$$O_2SO_3^-W_{0-1} \cdot O_3 \rightarrow O_3SO_3^-W_{0-1} + O_2 \qquad \text{(R10)}$$

is ca. 174 $kJ\,mol^{-1}$ exothermic. The de- and monohydrated $O_3SO_3^-$ structures are shown in the Supplement.

The two transition states of Reaction (R10) were then determined, and the monohydrated structure is shown in Fig. 5a. Besides the absent water molecule, the dehydrated structure differs only slightly from the monohydrated and is shown in the Supplement. However, considering the barrier heights, the effect of water is very significant. At standard conditions the de- and monohydrated energy barriers are 28.8 and 35.1 $kJ\,mol^{-1}$ respectively, implying that the water is significantly hindering the oxygen transfer due to destabilisation of the transition state (see Fig. 3). Finally, the pre-factors (Eq. 2) were determined to $3.12\times10^{10}\,s^{-1}$ and $7.40\times10^{9}\,s^{-1}$ respectively.

The reaction rate constant of Reaction (R10) was readily determined from Eq. (1) using the parameters described above (see Fig. 4). It is thus clear that the water molecule, while favouring charge transfer, effectively is hindering the oxidation of $O_2SO_3^-$. The main reason is the increased energy barrier.

To our knowledge $O_3SO_3^-$ has not previously been described in the literature, nor has it been observed in

experiments or in field studies. This suggests that $O_3SO_3^-$ is reactive and has too short of a lifetime to allow for observation. We therefore proceeded to investigate the possible decomposition of $O_3SO_3^-$ via

$$O_3SO_3^- W_{0-1} \rightarrow SO_4^- W_{0-1} + O_2. \quad \text{(R11)}$$

The monohydrated transition state is shown in Fig. 5b, and the dehydrated transition state is shown in the Supplement. We hereby determine the energy barrier to ca. 13 kJ mol^{-1} at standard conditions, practically independent of hydration (see Fig. 3). Since the energy release of Reaction (R10) is so much larger than the energy barrier, it is evident that Reaction (R11) is almost instantaneous.

3.4 Overall catalytic turnover

The presence of an ion-catalysed SO_2 oxidation cycle is of interest since an extra source of atmospheric H_2SO_4 significantly may alter the conditions for aerosol particle formation and growth. Although this assessment is the overall goal of this line of studies, several unresolved factors remain.

Considering the real atmosphere the most noticeable shortcoming is the influence of CO_2. This is known to be the dominant sink of O_3^- via

$$O_3^- + CO_2 \rightarrow CO_3^- + O_2. \quad \text{(R12)}$$

and cannot be neglected in any realistic model (Dotan et al., 1977; Luts and Parts, 2002). The chemical fate of CO_3^- is uncertain although the reaction

$$CO_3^- + SO_2 \rightarrow CO_2 + SO_3^- \quad \text{(R13)}$$

is known to proceed at collision rates, similar to Reaction (R2) (Fehsenfeld and Ferguson, 1974). However, extending the catalytic cycle in Fig. 1 to include these reactions is beyond the scope of this study.

Presently, we are able to assess the overall catalytic turnover in CO_2-free atmospheres, including most of the until now conducted chamber studies of ion-induced nucleation. Taking all investigated clusters, their relative concentrations, and all reactions into account, we find that the probability for cluster decomposition through Reaction (R3b) is 10^5–10^6 times more likely than other reactions between $O_3SO_3^- W_{0-1}$ and O_3. Details are presented in the Supplement. This thus suggests that each free electron may induce up to 10^5–10^6 SO_2 oxidations in atmospheres consisting of N_2, O_2, O_3, H_2O and SO_2 only.

This is consistent with recent experimental results from Enghoff et al. (2012). In the absence of UV light, it was found that each electron yielded a production of 10^6 sulfates in atmospheres heavily enriched in SO_2 and O_3. Further it was found that the isotopic fingerprint of this ion-produced sulfate was very different of sulfate from UV-induced SO_2 oxidation, clearly pointing at two different chemical mechanisms.

More commonly chamber atmospheres are made to resemble typical atmospheric conditions, and hence various pollutants become important. In those cases, the catalytic cycle may be terminated by mechanisms different from the ones presented so far, most likely involving species different from SO_2 and O_3. Considering, for example, a collision between $O_3^-(H_2O)_n$ and a NO_2 radical, this will rapidly be oxidized to NO_3^- with large energy gain,

$$O_3^- W_n + NO_2 \rightarrow NO_3^- W_n + O_2. \quad \text{(R14)}$$

Due to the stability of NO_3^-, the catalytic cycle for that particular electron is most likely terminated. Other potential scavengers include any species in which an electron may be more stabilized than on O_3^- or $O_2SO_3^-$, either through immediate charge transfer or after some chemical reaction. These may include radicals and acids, NO_x, cations and pre-existing aerosol particles or molecular clusters. Typically, NO_x and HNO_3 will be the dominant electron scavengers.

We here outline two methods of determining the rate of ion-induced H_2SO_4 formation. Most simply, if the actual concentrations of the involved ions are known, the rate of ion-induced H_2SO_4 formation may be determined based on the mechanism outlined in Fig. 1. Assuming $[O_3] \gg [SO_2]$ we obtain

$$r_{\text{ion cat.}} = Z \times [O_3^-(H_2O)_n] \times [SO_2], \quad (4)$$

where Z denotes the collision rate.

Alternatively, the ion-induced H_2SO_4 formation rate may be determined by realising that the incoming flux of electrons, J_{ion}, is the primary limiting factor. As shown in Fig. 1, the electron will remain catalytically active until scavenged, which occurs when the ionic cluster is hit by a scavenger. Again assuming $[O_3] \gg [SO_2]$ and that NO_x and HNO_3 are the dominant scavengers, the average number of catalytic cycles per electron is thus determined as

$$\text{Avg.cyc.} = \frac{Z(SO_2)}{Z(\text{electron scavenger})} \quad (5)$$

$$\sim \frac{[SO_2]}{[NO_x] + [HNO_3],} \quad (6)$$

where Z denotes the collision rate. The overall catalytic efficiency is then given as

$$r_{\text{ion cat.}} = J_{\text{ion}} \times \text{Avg.cyc.} \quad (7)$$

We now proceed to evaluate the relevance of ion-catalysed SO_2 oxidation in a typical CO_2-free chamber. Since we have no data for the ionic concentrations, we will use the latter approach. The well-known UV-induced H_2SO_4 production rate via Reaction (R1) is

$$r_{UV} = k_{UV} \times [OH] \times [SO_2], \quad (8)$$

where $k_{UV} = 1.3 \times 10^{-12}$ cm^3 molecule^{-1} s^1 (Atkinson et al., 2004).

We here assume the following conditions: [OH] = $5 \times 10^5\,cm^{-3}$ (day and night average), [NO_x] + [HNO_3] = 10 ppt = $2.5 \times 10^8\,cm^{-3}$ (pristine), [SO_2] = 5 ppb = $1.25 \times 10^{11}\,cm^{-3}$, [$O_3$] $\gg$ [SO_2], and $J_{ion} = 5$ ion pairs $cm^{-3}\,s^{-1}$ (middle or lower troposphere). We thus obtain Avg.cyc. = 500, and further obtain the contribution of H_2SO_4 from ion catalysis as

$$\frac{[H_2SO_4]_{\text{ion cat.}}}{[H_2SO_4]_{\text{total}}} = \frac{r_{\text{ion cat.}}}{r_{\text{ion cat.}} + r_{\text{UV}}} = 2.5\%. \quad (9)$$

Obviously, this is merely a rough estimate intended mainly as an illustrative example. However, variations in [H_2SO_4] on the order of a few percent are important, and the lack of this contribution in models of gaseous sulfur chemistry may lead to significant inaccuracies in predicting aerosol formation and growth rates.

4 Conclusions

It has previously been determined that de- or monohydrated clusters of $O_2SO_3^-$ are natural products of free atmospheric electrons. We have investigated the chemical fate of $O_2SO_3^-$ after various reactions with O_3.

We find two major reaction mechanisms leading to fundamentally different products, shown in Fig. 3. The first mechanism is a normal oxidation eventually leading to SO_4^- with large energy gain. However, significant energy barriers must be overcome, and we find that this reaction is of minor importance. Of primary importance is the transfer of the electron from $O_2SO_3^-$ to O_3. In the dehydrated system this is distinctly endothermic but still requires a lower energy than crossing the energy barrier of oxidation. In the hydrated systems, the water molecule can transfer with the charge from $O_2SO_3^-(H_2O)$ to $O_3^-(H_2O)$. We find that this path is 10^5 to 10^6 times more probable than $O_2SO_3^-(H_2O)$ oxidation. This reaction closes a catalytic cycle of SO_2 oxidation shown in Fig. 1. Both the chemical mechanism and the catalytic turnover number are in accordance with a recent chamber study by Enghoff et al. (2012).

Considering also the concentrations of other typical reactants, we conclude that the cycle is more probable to terminate due to reactions with an electron scavenger, most likely NO_x or HNO_3, than due to its own inherent side reactions. We are unable to assess the influence of this cycle in the real atmosphere, most noticeable due to CO_2. In chamber studies under UV exposure and in realistic gas mixtures, we roughly estimate the contribution of ion-catalysed H_2SO_4 to be on the order of several percent.

Besides being a source of atmospheric H_2SO_4, we note that the previously unknown origin of both $O_2SO_3^-$ and SO_4^-, seen in several experiments and field studies, readily is explained through this mechanism. Finally, this mechanism is also in accordance with the absence of SO_6^- from any observations since it explains why SO_6^- immediately decomposes to SO_4^- and O_2.

Supplementary material related to this article is available online at: http://www.atmos-chem-phys.net/13/3695/2013/acp-13-3695-2013-supplement.pdf.

Acknowledgements. The authors thank the Academy of Finland for funding and the CSC IT Centre for Science in Espoo, Finland, for computer time. We acknowledge the Villum foundation, University of Helsinki Chancellors travel grant, the Academy of Finland (CoE Project No. 1118615, LASTU Project No. 135054), ERC Project No. 257360-MOCAPAF for funding. We finally thank Martin B. Enghoff and Henrik Svensmark for valuable comments.

Edited by: A. Laaksonen

References

Adler, T. B., Knizia, G., and Werner, H. J.: A simple and efficient CCSD (T)-F12 approximation, J. Chem. Phys., 127, 221106, doi:10.1063/1.2817618, 2007.

Arnold, D., Xu, C., Kim, E., and Neumark, D.: Study of low-lying electronic states of ozone by anion photoelectron spectroscopy of O, J. Chem. Phys., 101, 912–922, 1994.

Atkinson, R., Baulch, D. L., Cox, R. A., Crowley, J. N., Hampson, R. F., Hynes, R. G., Jenkin, M. E., Rossi, M. J., and Troe, J.: Evaluated kinetic and photochemical data for atmospheric chemistry: Volume I – gas phase reactions of O_x, HO_x, NO_x and SO_x species, Atmos. Chem. Phys., 4, 1461–1738, doi:10.5194/acp-4-1461-2004, 2004.

Billing, G. D. and Mikkelsen, K. V.: Introduction to molecular dynamics and chemical kinetics, Wiley, New York, 1996.

Bondybey, V. and Beyer, M.: How many molecules make a solution?, Int. Rev. Phys. Chem., 21, 277–306, 2002.

Bork, N., Kurtén, T., Enghoff, M. B., Pedersen, J. O. P., Mikkelsen, K. V., and Svensmark, H.: Structures and reaction rates of the gaseous oxidation of SO_2 by an $O_3^-(H_2O)_{0-5}$ cluster – a density functional theory investigation, Atmos. Chem. Phys., 12, 3639–3652, doi:10.5194/acp-12-3639-2012, 2012a.

Bork, N., Kurtén, T., Enghoff, M. B., Pedersen, J. O. P., Mikkelsen, K. V., and Svensmark, H.: Ab initio studies of $O_2^-(H_2O)_n$ and $O_3^-(H_2O)$n anionic molecular clusters, $n \leq 12$, Atmos. Chem. Phys., 11, 7133–7142, doi:10.5194/acp-11-7133-2011, 2011b.

Boys, S. F. and Bernardi, F: Calculation of Small Molecular Interactions by Differences of Separate Total Energies – Some Procedures with Reduced Errors, Molecular Physics., 19, 553–566, 1970.

Carslaw, K., Harrison, R. G., and Kirkby, J.: Cosmic rays, clouds, and climate, Science, 298, 1732–1737, doi:10.1126/science.1076964, 2002.

Dobrin, S., Boo, B., Alconcel, L., and Continetti, R.: Photoelectron Spectroscopy of SO_3^- at 355 and 266 nm, J. Phys. Chem. A, 104, 10695–10700, 2000.

Dotan, I., Davidson, J. A., Streit, G.E. Albritton, D., and Fehsenfeld, F.: A study of the reaction O_3^- + CO_2 ↔ CO_3^- + O_2 and its implication on the thermochemistry of CO_3 and O_3 and their negative ions, J. Chem. Phys., 67, 2874–2879, 1977.

Dunning, T. H. J.: Gaussian basis sets for use in correlated molecular calculations. I. The atoms boron through neon and hydrogen, J. Chem. Phys., 90, 1007–1023, doi:10.1063/1.456153, 1989.

Ehn, M., Junninen, H., Petäjä, T., Kurtén, T., Kerminen, V.-M., Schobesberger, S., Manninen, H. E., Ortega, I. K., Vehkamäki, H., Kulmala, M., and Worsnop, D. R.: Composition and temporal behavior of ambient ions in the boreal forest, Atmos. Chem. Phys., 10, 8513–8530, doi:10.5194/acp-10-8513-2010, 2010.

Elm, J., Bilde, M., and Mikkelsen, K. V.: Assessment of Density Functional Theory in Predicting Structures and Free Energies of Reaction of Atmospheric Prenucleation Clusters, Journal of Chemical Theory and Computation, 8, 2071–2077, 2012.

Enghoff, M. B., Bork, N., Hattori, S., Meusinger, C., Nakagawa, M., Pedersen, J. O. P., Danielache, S., Ueno, Y., Johnson, M. S., Yoshida, N., and Svensmark, H.: An isotopic analysis of ionising radiation as a source of sulphuric acid, Atmos. Chem. Phys., 12, 5319–5327, doi:10.5194/acp-12-5319-2012, 2012.

Enghoff, M. B. and Svensmark, H.: The role of atmospheric ions in aerosol nucleation – a review, Atmos. Chem. Phys., 8, 4911–4923, doi:10.5194/acp-8-4911-2008, 2008.

Fehsenfeld, F. C. and Ferguson, E. E.: Laboratory studies of negative ion reactions with atmospheric trace constituents, J. Chem. Phys., 61, 3181–3193, doi:10.1063/1.1682474, 1974.

Gleason, J.: Chemical ionization detection of $HOSO_2$ and the kinetics of the reaction of $HOSO_2$ + 0_2, Ph.D. dissertation, Univ. of Colorado, USA, 1987.

Hänggi, P., Talkner, P., and Borkovec, M.: Reaction-rate theory: fifty years after Kramers, Rev. Modern Phys., 62, 251–342, 1990.

Kazil, J., Stier, P., Zhang, K., Quaas, J., Kinne, S., O'Donnell, D., Rast, S., Esch, M., Ferrachat, S., Lohmann, U., and Feichter, J.: Aerosol nucleation and its role for clouds and Earth's radiative forcing in the aerosol-climate model ECHAM5-HAM, Atmos. Chem. Phys., 10, 10733–10752, doi:10.5194/acp-10-10733-2010, 2010.

Keesee, R., Lee, N., and Castleman Jr., A.: Properties of clusters in the gas phase. 3. Hydration complexes of carbonate (1-) and bicarbonate (1-) ions, Journal of the American Chemical Society, 101, 2599–2604, 1979.

Kirkby, J., Curtius, J., Almeida, J., Dunne, E., Duplissy, J., Ehrhart, S., Franchin, A., Gagné, S., Ickes, L., Kürten, A., Kupc, A., Metzger, A., Riccobono, F., Rondo, L., Schobesberger, S., Tsagkogeorgas, G., Wimmer, D., Amorim, A., Bianchi, F., Breitenlechner, M., David, A., Dommen, J., Downard, A., Ehn, M., Flagan, R. C., Haider, S., Hansel, A., Hauser, D., Jud, W., Junninen, H., Kreissl, F., Kvashin, A., Laaksonen, A., Lehtipalo, K., Lima, J., Lovejoy, E. R., Makhmutov, V., Mathot, S., Mikkilä, J., Minginette, P., Mogo, S., Nieminen, T., Onnela, A., Pereira, P., Petäjä, T., Schnitzhofer, R., Seinfeld, J. H., Sipilä, M., Stozhkov, Y., Stratmann, F., Tomé, A., Vanhanen, J., Viisanen, Y., Vrtala, A., Wagner, P. E., Walther, H., Weingartner, E., Wex, H., Winkler, P. M., Carslaw, K. S., Worsnop, D. R., Baltensperger, U., and Kulmala, M.: Role of sulphuric acid, ammonia and galactic cosmic rays in atmospheric aerosol nucleation, Nature, 476, 429–435, 2011.

Kulmala, M., Vehkamäki, H., Petäjä, T., Dal Maso, M., Lauri, A., Kerminen, V., Birmili, W., and McMurry, P.: Formation and growth rates of ultrafine atmospheric particles: a review of observations, J. Aerosol Sci., 35, 143–176, 2004.

Kupiainen, O., Ortega, I. K., Kurtén, T., and Vehkamäki, H.: Amine substitution into sulfuric acid – ammonia clusters, Atmos. Chem. Phys., 12, 3591–3599, doi:10.5194/acp-12-3591-2012, 2012.

Kurtén, T., Ortega, I. K., and Vehkamáki, H.: The sign preference in sulfuric acid nucleation, Journal of Molecular Structure: THEOCHEM, 901, 169–173, 2009.

Li, W. and McKee, M.: Theoretical Study of OH and H2O Addition to SO_2, J. Phys. Chem. A, 101, 9778–9782, 1997.

Lovejoy, E., Curtius, J., and Froyd, K.: Atmospheric ion-induced nucleation of sulfuric acid and water, J. Geophys. Res., 109, D08204, doi:10.1029/2003JD004460, 2004.

Luts, A. and Parts, T.: Evolution of negative small air ions at two different temperatures, J. Atmos. Sol.-Terr. Phys., 64, 763–774, 2002.

Mauldin III, R., Berndt, T., Sipilä, M., Paasonen, P., Petäjä, T., Kim, S., Kurtén, T., Stratmann, F., Kerminen, V., and Kulmala, M.: A new atmospherically relevant oxidant of sulphur dioxide, Nature, 488, 193–196, 2012.

Möhler, O., Reiner, T., and Arnold, F.: The formation of $S0_5^-$ by gas phase ion-molecule reactions, J. Chem. Phys., 97, 8233–8239, 1992.

Morokuma, K. and Muguruma, C.: Ab initio molecular orbital study of the mechanism of the gas phase reaction SO_3 + H_2O: importance of the second water molecule, Journal of the American Chemical Society, 116, 10316–10317, 1994.

Mulliken, R.: Electronic Population Analysis on LCAO-MO Molecular Wave Functions, J. Chem. Phys., 23, 1831–1840, doi:10.1063/1.1740588, 1955.

Nadykto, A. B., Al Natsheh, A., Yu, F., Mikkelsen, K. V., and Ruuskanen, J.: Quantum nature of the sign preference in ion-induced nucleation, Phys. Rev. Lett., 96, 125701, doi:10.1103/PhysRevLett.96.125701, 2006.

Nieminen, T., Manninen, H., Sihto, S., Yli-Juuti, T., Mauldin, III, R., Petaja, T., Riipinen, I., Kerminen, V., and Kulmala, M.: Connection of sulfuric acid to atmospheric nucleation in boreal forest, Environ. Sci. Technol., 43, 4715–4721, 2009.

Novick, S., Engelking, P., Jones, P., Futrell, J., and Lineberger, W.: Laser photoelectron, photodetachment, and photodestruction spectra of O_3^-, J. Chem. Phys., 70, 2652, doi:10.1063/1.437842, 1979.

Ortega, I. K., Kupiainen, O., Kurtén, T., Olenius, T., Wilkman, O., McGrath, M. J., Loukonen, V., and Vehkamäki, H.: From quantum chemical formation free energies to evaporation rates, Atmos. Chem. Phys., 12, 225–235, doi:10.5194/acp-12-225-2012, 2012.

Payzant, J., Yamdagni, R., and Kebarle, P.: Hydration of CN-, NO-2-, NO3-, and OH-in the Gas Phase, Can. J. Chem., 49, 3308–3314, 1971.

Peach, M. J. G., Helgaker, T., Sałek, P., Keal, T. W., Lutnæs, O. B., Tozer, D. J., and Handy, N. C.: Assessment of a Coulomb-attenuated exchange–correlation energy functional, Phys. Chem. Chem. Phys., 8, 558–562, 2006.

Peterson, K. A., Adler, T. B., and Werner, H. J.: Systematically convergent basis sets for explicitly correlated wavefunctions: The atoms H, He, B–Ne, and Al–Ar, J. Chem. Phys., 128, 084102, doi:10.1063/1.2831537, 2008.

Rosenfeld, D.: Aerosols, clouds, and climate, Science, 312, 1323–1324, 2006.

Simpson, J. and Wiggert, V.: Models of precipitating cumulus towers, Mon. Weather Rev., 97, 471–489, 2009.

Sipilä, M., Berndt, T., Petäjä, T., Brus, D., Vanhanen, J., Stratmann, F., Patokoski, J., Mauldin III, R., Hyvärinen, A., Lihavainen, H., and Kulmala, M.: The role of sulfuric acid in atmospheric nucleation, Science, 327, 1243–1246, 2010.

Sorokin, A. and Arnold, F.: Laboratory study of cluster ions formation in H_2SO_4-H_2O system: Implications for threshold concentration of gaseous H_2SO_4 and ion-induced nucleation kinetics, Atmos. Environ., 41, 3740–3747, 2007.

Sorokin, A. and Arnold, F.: Analysis of experiments on ion-induced nucleation and aerosol formation in the presence of UV light and ionizing radiation, Atmos. Environ., 43, 3799–3807, 2009.

Spracklen, D. V., Bonn, B., and Carslaw, K. S.: Boreal forests, aerosols and the impacts on clouds and climate, Philosophical Transactions of the Royal Society A: Mathematical, Phys. Eng. Sci., 366, 4613–4626, doi:10.1098/rsta.2008.0201, 2008.

Su, T. and Bowers, M.: Theory of ion-polar molecule collisions. Comparison with experimental charge transfer reactions of rare gas ions to geometric isomers of difluorobenzene and dichloroethylene, J. Chem. Phys., 58, 3027–3037, doi:10.1063/1.1679615, 1973.

Svensmark, H., Pedersen, J. O. P., Marsh, N. D., Enghoff, M. B., and Uggerhøj, U. I.: Experimental evidence for the role of ions in particle nucleation under atmospheric conditions, Proceedings of the Royal Society A: Mathematical, Phys. Eng. Sci., 463, 385–396, doi:10.1098/rspa.2006.1773, 2007.

Tohmfor, G. and Volmer, M.: Annalen der Physik, 426, 446–448, doi:10.1002/andp.19394260503, 1939.

Welz, O., Savee, J., Osborn, D., Vasu, S., Percival, C., Shallcross, D., and Taatjes, C.: Direct Kinetic Measurements of Criegee Intermediate (CH_2OO) Formed by Reaction of CH_2I with O_2, Science, 335, 204–207, 2012.

Wiedensohler, A., Cheng, Y., Nowak, A., Wehner, B., Achtert, P., Berghof, M., Birmili, W., Wu, Z., Hu, M., Zhu, T., Takegawa, N., Kita, K., Kondo, Y., Lou, S. R., Hofzumahaus, A., Holland, F., Wahner, A., Gunthe, S. S., Rose, D., Su, H., and Pöschl, U.: Rapid aerosol particle growth and increase of cloud condensation nucleus activity by secondary aerosol formation and condensation: A case study for regional air pollution in northeastern China, J. Geophys. Res., 114, D00G08, doi:10.1029/2008JD010884, 2009.

Yanai, T., Tew, D. P., and Handy, N. C.: A new hybrid exchange-correlation functional using the Coulomb-attenuating method (CAM-B3LYP), Chem. Phys. Lett., 393, 51–57, 2004.

Yu, F. and Luo, G.: Simulation of particle size distribution with a global aerosol model: contribution of nucleation to aerosol and CCN number concentrations, Atmos. Chem. Phys., 9, 7691–7710, doi:10.5194/acp-9-7691-2009, 2009.